2025 International Conference on Advanced Mechatronics and Intelligent Energy Systems

Design of High Performance Bandgap Reference Voltage Circuit

AIPCP25-CF-AMIES2025-00051 | Article

Design of High Performance Bandgap Reference Voltage Circuit

Jingcheng Gu

College of Integrated Circuit Science and Engineering (College of Industry-Education Integration), Nanjing University of Posts and Telecommunications ,Jiangsu ,210023 ,China

b22030823@njupt.edu.cn

Abstract. The bandgap reference voltage circuits serves as the "precision heart" of analog integrated circuits, with performance advancements and design innovations being essential challenges in advancing high-precision electronic systems towards minimal temperature drift and enhanced stability. This study begins with an examination of the thermal voltage properties of bipolar transistors, methodically determining the temperature compensation technique for reference voltage. It elucidates the intrinsic limitations of conventional circuits regarding temperature nonlinearity, process sensitivity, and driving capability. By integrating contemporary design examples, we discuss the substantial improvement in temperature coefficient and noise performance achieved through higher-order nonlinear compensation techniques and wide dynamic range current mirrors. Additionally, we delineate the topological distinctions between op-amp outputs and traditional architectures through comparative analysis. Through the analysis of the topological distinctions between operational amplifier outputs and conventional architectures, we have elucidated the trade-off strategies of various designs concerning area efficiency, robustness, and power supply rejection ratio, thereby offering theoretical support for optimization across multiple scenarios. In the future, the profound integration of advanced processes and adaptive compensation algorithms will enable bandgap reference circuits to pioneer advancements in sub-1V ultra-low-voltage design, extreme environmental resilience, and multi-physical-field co-optimization, establishing them as a dependable foundation for intelligent electronic systems.

INTRODUCTION

Substantial advancements have been achieved in the investigation of bandgap reference voltage circuits, which are essential components of analogue integrated circuits, particularly in the areas of low temperature drift design, low voltage working state, and high power supply rejection ratio (PSRR). Nevertheless, gaps persist, including limitations in multi-parameter co-optimization, inadequate adaptability to harsh settings, and issues with advanced process compatibility. The primary academic concerns include temperature nonlinearity compensation, self-suppression of process deviations, and the investigation of multi-physical field coupling effects. The objective of this study domain is to devise adaptive compensation methodologies that reconcile low temperature drift, high power supply rejection ratio (PSRR), and minimal power usage, while enhancing robustness in dynamic environments and sophisticated processes. This research is significant for establishing dependable benchmarks for high-precision analogue systems, advancing applications in the Internet of Things and automotive electronics, and fostering multidisciplinary cross-innovation.

This paper aims to systematically elucidate the fundamental principles and design methodologies of bandgap reference voltage circuits, while also identifying optimisation trajectories for existing technologies across various application contexts through a comprehensive analysis of typical circuit architectures. The work elucidates the temperature adjustment method of bandgap reference voltage based on the thermal voltage characteristics of bipolar transistors, while examining the issues of temperature nonlinearity and process deviation sensitivity inherent in traditional architectures. Concurrently, by integrating contemporary design cases, the research investigates the ameliorative impact of innovative techniques, such as higher-order nonlinear compensation and wide dynamic range

current mirrors, on temperature coefficients, noise performance, and power supply rejection ratios. This study aims to delineate the fundamental characteristics of superior circuit designs by comparing the disparities in driving capability, area efficiency, and robustness across various circuit topologies, thereby offering a comprehensive analytical framework for the theory and application of high-precision reference voltage circuits.

PRINCIPLES OF BANDGAP REFERENCE VOLTAGE

The fundamental concept of bandgap reference voltage is to combine two voltage quantities with opposing temperature coefficients and assign appropriate weights to achieve a voltage value that is relatively stable during temperature fluctuations, which is referred to as the reference voltage [1][2]. It is possible to infer that the voltage with a positive temperature coefficient is signified as V+, while the voltage with a negative temperature coefficient is signified as V-. There are unspecified design parameters α and β that are satisfied:

$$\alpha \cdot \frac{\partial V_+}{\partial T} + \beta \cdot \frac{\partial V_-}{\partial T} = 0 \tag{1}$$

From this principle, the reference voltage can be expressed as:

$$V_{REF} = \alpha \cdot V_+ + \beta \cdot V_- \tag{2}$$

Bipolar transistors have the following characteristics: the base-emitter voltage (V_{BE}) is inversely proportional to absolute temperature, and the difference in base-emitter voltages between two bipolar transistors (ΔV_{BE}) is proportional to absolute temperature at varying collector currents. Also, Bipolar transistors provide benefits in transconductance matching, process consistency, and subthreshold application; their base-emitter voltage demonstrates greater resilience to process changes and temperature fluctuations compared to MOS devices **Error! Reference source not found.**. As a result, bipolar transistors can serve as the basis for a bandgap voltage reference, functioning as both a negative temperature coefficient voltage and a positive temperature coefficient voltage **Error! Reference source not found.**.

Negative Temperature Coefficient Voltage

The collector current and base-emitter voltage of a bipolar transistor are satisfied:

$$I_S = I_C \exp(V_{BE}/V_T) \tag{3}$$

Express V_{BE} in terms of the saturation current I_S, collector current I_C, and thermal voltage of a bipolar transistor V_T;$V_T = kT/q$, k represents Boltzmann's constant, and q represents the electron charge;The negative temperature coefficient is then obtained by taking the partial derivative of V_{BE} with respect to the absolute temperature T:

$$\frac{\partial V_{BE}}{\partial T} = \frac{V_{BE} - (m+4)V_T - E_g/q}{T} \tag{4}$$

where m ≈ 1.5 and Eg = 1.12 eV is the bandgap energy of silicon. When V_{BE} ≈750 mV and T=300 K,∂T≈-1.5mV/℃ .The size of the positive temperature coefficient, as indicated in Eq. (4), varies with absolute temperature and can only be ascertained when the absolute temperature is known. A bandgap reference with a zero temperature coefficient may only be produced at a certain absolute temperature point **Error! Reference source not found.**.

Positive Temperature Coefficient Voltage

Assume that the bias currents of two transistors of the same size are nI_0 and I_0, and that the difference between their base-emitter voltages is:

$$\Delta V_{BE} = V_{BE1} - V_{BE2} = V_T \ln \frac{nI_0}{I_{S1}} - V_T \ln \frac{I_0}{I_{S2}} = V_T \ln n \tag{5}$$

Take the partial derivative of ΔV_{BE} with respect to the absolute temperature:

$$\frac{\partial \Delta V_{BE}}{\partial T} = \frac{k}{q} \ln n > 0 \tag{6}$$

ΔV_{BE} demonstrates positive temperature properties.

Bandgap Reference Voltage

Using V_{BE} and ΔV_{BE}, a reference voltage with zero temperature coefficient can be designed:

$$V_{REF} = \alpha \cdot V_{BE} + \beta \cdot V_T \ln n \tag{7}$$

When ≈750mV, T=300K, $\partial V_{BE}/\partial T$ ≈-1.5mV/, $\partial V_T/\partial T$ ≈0.087mV/, and let the weight α=1, the obtained condition is:

$$\beta \cdot \ln n \approx 17.2 \tag{8}$$

Conventional circuit of Bandgap Voltage Reference

The fundamental construction of a bandgap circuit comprises a general current mirror, a bandgap reference source core, an amplifier, a bipolar transistor, and resistors. Figure 1 illustrates a standard bandgap reference voltage circuit.

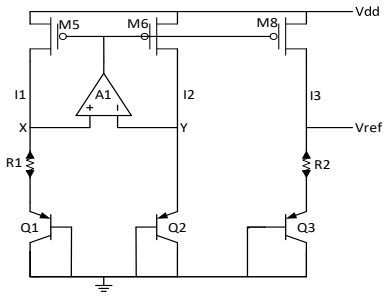

FIGURE 1. Conventional bandgap reference voltage circuit

In the circuit, tubes M5, M6, and M8 form a current mirror and the dimensions of the three tubes are satisfied:

$$\left(\frac{W}{L}\right)_5 = \left(\frac{W}{L}\right)_6 = \frac{1}{M} \cdot \left(\frac{W}{L}\right)_8 \tag{9}$$

Then the current flowing through them satisfies:

$$I_1 = I_2 = \frac{I_3}{M} \tag{10}$$

According to Eq. (10), the currents in Q1 and Q2 are identical, n is the ratio of the number of Q1 and Q2 tubes arranged in parallel.Then the Q1 and Q2 base-emitter voltage difference satisfies Eq. (5).The virtual short characteristic of op-amp A1 leads the potentials at nodes X and Y to be the identical, therefore the amount of the voltage drop across resistor R1 is equal to ΔV_{BE} . The leakage currents flowing through M5, M6, and M8 are:

$$I_1 = I_2 = \frac{V_T \cdot \ln n}{R_1} = \frac{I_3}{M} \tag{11}$$

I_3 represents the PTAT current acquired by recreating the current flowing through R1 using the current mirror. The PTAT voltage obtained by flowing through R2 is added to the base emitter of Q3 tube to obtain the reference output voltage:

$$V_{REF} = V_{BE,\ Q3} + M \cdot \frac{R_2}{R_1} \cdot V_T \ln n \tag{12}$$

Combining Eq. (8) yields:

$$M \cdot \frac{R_2}{R_1} \cdot \ln n \approx 17.2 \tag{13}$$

Approaching the aforementioned equation, a reference bandgap voltage exhibiting a zero temperature coefficient at T=300K can be generated, and the dimensions and thermal properties of the reference voltage could be modified by altering the n value.

Traditional bandgap reference voltage circuits may provide a zero temperature coefficient bandgap reference voltage directly and effectively; nevertheless, they possess several limitations. The base-emitter voltage of a practical bipolar transistor possesses a high-order nonlinear temperature characteristic, resulting in curvature errors in the reference voltage across a broad temperature spectrum. This nonlinearity is insufficiently compensated by traditional architectures, thereby constraining its stability in extreme temperature conditions. In the quest for a stable bandgap reference source approaching perfection, several derivative circuits have been developed.

Create a reference voltage through the operational amplifier's output stage. With the circuit of Figure 2, a bandgap reference voltage can be generated directly at the output of the operational amplifier.

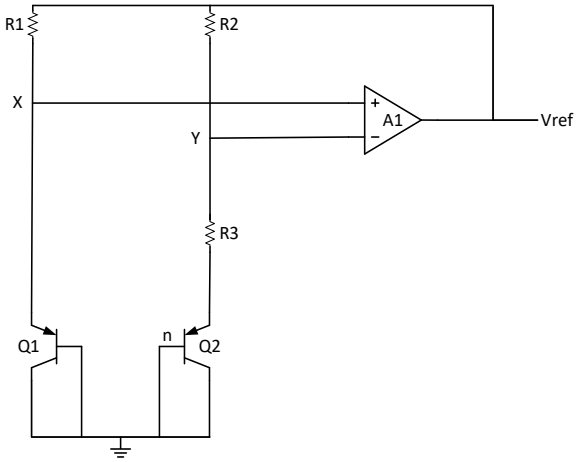

FIGURE 2. Circuit diagram for generating reference voltage at the output of op amp

The fictitious short characteristic of op-amp A1 renders the potentials at nodes X and Y equivalent, and given that resistor R1 equals R2, the currents traversing transistors Q1 and Q2 are same.Q1 and Q2 are transistors of the same specification with bias currents nI_0 and I_0, respectively, then the difference between the base-emitter voltages of Q1 and Q2 satisfies Eq. (5), with n representing the ratio of the number of Q2 and Q1 tubes connected in parallel. The voltage at the output of operational amplifier A1 is:

$$V_{REF} = V_{BE,\ Q2} + \frac{R_2+R_3}{R_3} \cdot V_T \ln n \tag{14}$$

Combined with Eq. (8), if $\frac{R_2+R_3}{R_3} \cdot lnn \approx 17.2$ is satisfied, a bandgap reference voltage at T=300K can be obtained. The figure 3 illustrates the feedback loop of the bandgap voltage reference utilized in the reference voltage circuit, which produces the reference voltage at the output of the operational amplifier.

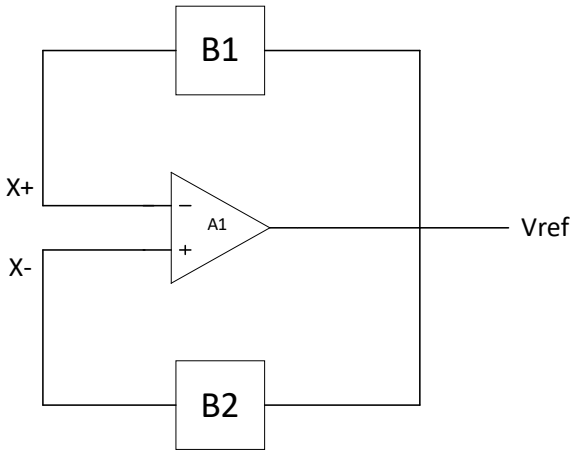

FIGURE 3. System structure of bandgap reference source

In the structure diagram, A1 is an operational amplifier with a gain of A_{V1}; R_1 and Q_1 form a divider network B_1 with a gain of β_1 ; R_2 , R_3 and Q_1 form a divider network B_2 with a gain of β_2 . When the gain of the amplifier is large enough, the transfer function to the system is deformed:

$$\frac{V_{REF}}{X_+ - X_-} = \frac{A_{V1}}{1 + A_{V1}(\beta_1 - \beta_2)} \approx \frac{1}{(\beta_1 - \beta_2)} \tag{15}$$

The closed loop gain of the circuit is:

$$|A|_{closed-loop} = \left|\frac{1}{\beta_1 - \beta_2}\right| \tag{16}$$

β_1 and β_2 respectively take the values of $|\beta_1| = R_Q/R_1 + R_Q$, $|\beta_2| = R_3 + R_Q/R_3 + R_Q$,

A correlation exists between resistors R2, R3, and the ratio of the quantity of parallel bipolar transistors, n:$R_1 = R_2 = \left(\frac{17.2}{lnn} - 1\right) R_3$.The equivalent resistance of the emitter of transistor Q to ground can be expressed as:$R_Q = V_T/I_C = R_3/lnn$, Simplified closed-loop gain has:

$$|A|_{closed-loop} = \frac{(R_2 + R_3 + R_Q)(R_1 + R_Q)}{R_1 R_3} = \frac{18.2}{lnn}\left(1 + \frac{1}{17.2 - lnn}\right) \tag{17}$$

The overall gain of a conventional bandgap circuit, measured from the input of the error amplifier to the output of the reference voltage, is:

$$|A|_{total} = |A|_{closed-loop} \cdot g_{m8}(R_2 + R_{Q3}) = \frac{18.2}{lnn} \tag{18}$$

where g8 is the transconductance of the M8 tube in Figure. 1.To ensure the convenience of layout design and minimize the disparity in current ratio, the value of n is often kept relatively small. The comparison of Eq. (17) and Eq. (18) indicates that the closed-loop gain for producing the reference voltage at the output of the operational amplifier exceeds that of a traditional bandgap voltage reference.

Besides the disparity in closed-loop benefits, an examination of the two circuit architectures indicates that:

Conventional bandgap reference voltage circuits are incapable of directly powering following circuits; instead, a buffer must be interposed between the bandgap voltage reference and the subsequent circuits, with buffer providing the necessary power to these circuits [2].The rationale for this is that if subsequent circuits draw current directly from the output of this bandgap voltage reference, such current constitutes a component of the PTAT current. This is due to the fact that the power supply current demanded by the subsequent circuits is not inherently proportional to absolute temperature. Consequently, it cannot be assured that the current remains proportional to absolute

temperature when traversing resistor R2, which produces voltage references that lack temperature dependence, thereby compromising the functionality of the bandgap voltage reference. Subsequent alterations in supply current demands within circuits will directly influence the bandgap voltage reference's output voltage. Therefore, when utilizing this bandgap voltage reference configuration, it is crucial to implement a buffer to isolate the output of the bandgap voltage reference concurrently. Generating the reference voltage at the op-amp output does not necessitate buffer isolation, and its driving capacity surpasses that of traditional bandgap reference voltage circuits.

However, in contrast to the traditional bandgap reference voltage circuit, the circuit intended to provide the reference voltage at the op-amp output requires an increase in the resistance values of R1 and R2 for a minimal value of n. In CMOS technologies, passive resistors occupy substantial chip regions. Moreover, given identical values of n in both circuits, the circuit that creates the reference voltage at the output of the operational amplifier generates greater noise interference. This exemplifies the diverse characteristics of analog integrated circuit design.

CURVATURE CORRECTION PROBLEMS

The plot of bandgap voltage vs absolute temperature, generated by simulation tools, frequently exhibits curvature. This curvature indicates that the zero-temperature characteristic of the bandgap voltage is not invariant throughout a broad spectrum of temperature fluctuations. The temperature-dependent characteristics of the base-emitter voltage, collector current, and detuned voltage frequently influence this curvature.

Quite a few bandgap reference circuits have been developed utilizing curvature correction. Cheng Liang attains a further reduction in the temperature coefficient by engineering a circuit that produces a current proportional to the square of the absolute temperature, which is then superimposed on a standard bandgap reference source [6].

Chen Xiaolong incorporated a curve correction circuit into the conventional Brokaw structure, which extracts a portion of the temperature compensation current from the original current, specifically, the current exhibits a temperature-dependent escalation characteristic that matches the first-order temperature drift of the compensation reference voltage. As the temperature decreases, the current that diminishes with rising temperature is diverted, resulting in reduced current flow through the resistor. This action mitigates the variation of the reference voltage with temperature, thereby achieving effective curvature correction [7]. Liu Hui, on the other hand, employs subthreshold curvature compensation and chopper modulation techniques to address the higher order temperature term coefficient issue in bandgap references and the input misalignment problem in operational amplifiers. His bandgap reference circuit is designed utilizing the SMIC.18BCD process, which compensates for higher order nonlinear voltages in the bandgap voltage by enhancing the nonlinear currents produced in the circuit when a series-connected NMOS transistor operates in the subthreshold region [8].

A low-temperature-drift bandgap reference circuit featuring segmented curvature compensation, developed by Prof. Ma Arnin, represents a significant advancement in the field. The circuit implements a higher-order nonlinear curvature-compensated bandgap reference utilizing the SMIC-130 nm process. The circuit incorporates a segmented nonlinear curvature-compensated current-generating circuit, which addresses higher-order nonlinear terms, thereby compensating for temperature coefficients across both low and high-temperature segments. This design enables the BGR to operate effectively over a wide temperature range with a reduced temperature coefficient. At the same time, the circuit employs wide dynamic range current mirrors in place of conventional ones to enhance the accuracy of current replication. The simulation results indicate that the temperature coefficient decreased from 13.132×/°C to 1.1148×/°C following the implementation of compensation. The power supply rejection ratios are -46 dB for low frequency operation and -30 dB for high frequency operation. The equivalent output noise is 0.16 μV/ √(（Hz）). The design effectively attains a low temperature coefficient while managing circuit power consumption, making it appropriate for various wearable portable devices [9].

In practical application, the emphasis can be on three factors: temperature range limit testing, noise performance, and supply voltage adaptability. For extreme temperatures, accelerated life testing methods and increasing the temperature stress can be used to simulate prolonged operation at extreme temperatures. Based on theories such as the Arrhenius model, a suitable acceleration factor is determined to shorten the test time.

For noise handling, low noise coefficient resistor materials or unique resistor architectures might be utilized. A voltage monitoring and control chip can be used to monitor the input power supply voltage in real time and relay that information back to the control circuit, allowing for rapid changes.

DEVELOPMENT PROSPECT

The trajectory of future integrated circuit development is becoming evident, with chips aiming for enhanced integration and downsizing, reduced power consumption and improved energy efficiency, more accuracy and stability, as well as advanced intelligence and adaptive capabilities. As the central component of the analog system, the bandgap reference voltage circuit will remain one of the most important part. An integrated 7-bit voltage configurator and a digitally changeable bandgap reference voltage source were developed for use in 5G wireless communication systems employing a CMOS 180 nm technology in the consumer electronics industry. Due to its low temperature coefficient and strong power supply rejection ratio, the bandgap reference circuit offers a steady voltage for RF front-end and baseband chips, which is essential for 5G communications' improved power supply noise rejection needs [10];

The dynamic regulation of multiple power domains in folding screen cell phones necessitates additional bandgap circuits to accommodate a wide supply range and ensure rapid transient response [11]. In automotive electronics, the millimeter-wave radar receiving chain of automatic driving systems necessitates bandgap references to attain an initial accuracy of ±0.1%, thereby ensuring the quantization accuracy of the ADC/DAC. In the on-board battery management system, bandgap circuits regulate reference drift across a broader temperature range within 1mV through curvature compensation technology, ensuring reliable estimation of the battery's charging state. The research and development team at Tsinghua Fierce Lion is working on a 4D millimeter wave radar dataset for autonomous driving. The accuracy of its multi-modal data synchronization is dependent on the reference voltage's stability, which in turn depends on the multi-sensor fusion. A low temperature drift benchmark is also being considered [12][13]. In industrial automation, the long-term stability of the bandgap reference is crucial for the calibration accuracy of the transmitter. Additionally, its low-density characteristic of the noise spectrum significantly enhances the signal-to-noise ratio of the 24-bit high-precision ADC [14].

In aerospace applications, radiation-hardened bandgap circuits are developed utilizing bipolar-CMOS synergy to ensure minimal output voltage fluctuations during single particle bombardment, while also satisfying the continuous operation requirements of on-board equipment in extreme environments [15][16][17].With the advancement of FinFET processes, innovative bandgap architectures are surpassing the conventional 1.2V threshold, enabling programmable reference outputs ranging from 0.4V to 3.3V via multi-branch current-mode configurations[18]. The digital calibration module is deeply integrated, enabling compensation of the temperature nonlinearity error of the reference voltage to a ±5ppm level through backend algorithms.

In terms of low power consumption, people have achieved a significant reduction reaching the nA level or lower through the implementation of innovative structures and processes, including MOS tubes that function in the subthreshold region. This approach not only prolongs the operational lifespan of battery-operated devices but also offers robust support for applications that are highly sensitive to power usage, such as those found in the Internet of Things. Simultaneously, notable advancements have been achieved in critical performance metrics, including power supply rejection ratio (PSR) and temperature coefficient. The high-precision reference voltage circuits maintain a stable output voltage across a broad temperature range. This stability is essential for applications such as digital-to-analog converters and low-voltage-dropout linear voltage regulators, which necessitate high-precision reference voltages.

The incorporation of an overcurrent protection feature illustrates the progress of analog design regarding circuit safety. The capacity to promptly implement protective measures when the load current is above the predetermined threshold augments the dependability and stability of the overall system.

CONCLUSION

In the domain of integrated circuit analog design, bandgap reference circuits have attained remarkable outcomes. The accomplishments range from low-power reference voltage circuits to high-stability LDO circuits with overcurrent protection, as well as the design of low-power, low-temperature-drift bandgap reference sources, showcasing the exceptional capability of analog design to satisfy diverse application requirements. Simultaneously, these improvements propel analog design towards enhanced precision and increased flexibility, establishing a dependable voltage reference for electronic systems across many domains.

REFERENCES

1. B. Razavi, Analog CMOS Integrated Circuit Design. Xi'an: Xi'an Jiaotong University Press (2003).
2. Y. Wang and L.N. He, CMOS Low Dropout Linear Regulator. Beijing: Science Press (2012).
3. H. Rashidian, I. Soltani, and M. Maghsoudi, 2.69-ppm/°C curvature-compensated bandgap voltage reference based on BJT. Integr. VLSI J. **102**, 102361 (2025).
4. Y. Zhang, J. Wang, and H. Zhou, Design of a low temperature coefficient bandgap reference voltage source. Comput. Technol. Dev. **26**(2), 150-153+160 (2016).
5. S.M. Sze and K.K. Ng, Physics of Semiconductor Devices (3rd ed.). Xi'an: Xi'an Jiaotong University Press (2008).
6. L. Cheng, A novel second-order curvature compensation structure for bandgap reference sources. Shanxi Electron. Technol. **6**, 6-8+27 (2024).
7. S.L. Chen and Q.Y. Feng, Design of a low-power low-temperature-drift bandgap reference source. Microelectron. (2025).
8. H. Liu and X. Cao, Research and design of curvature-compensated chopper bandgap reference. J. Chengdu Inst. Technol. **28**(1), 37-43 (2025).
9. A. Ma, H. Guo, Z. Li, et al., A low-temperature-drift bandgap with segmental curvature compensation. Microelectron. (2025).
10. J. Lv and Q. Hu, Design of bandgap reference with curvature compensation. Electron. Packag. **16**(8), 34-36 (2016).
11. L. Hou, L. Zhang, T. Chen, et al., A second-order curvature-compensated zener reference voltage supply circuit. Chinese Patent CN202311552840 (2023).
12. L. Wang, et al., InterFusion: Interaction-based 4D Radar and LiDAR Fusion for 3D Object Detection. In: 2022 IEEE/RSJ Int. Conf. Intell. Robots Syst. (IROS) (2022).
13. D. Zhang, Y. Jiang, and M. Yu, Noise analysis based on bandgap reference source circuit. J. Electron. Meas. Instrum. **25**(12), 29-33 (2011).
14. Z. Liu, L. Yang, H. Yao, et al., Design of radiation hardened CMOS reference. J. Terahertz Sci. Electron. Inf. Technol. **15**(1), 125-128+133 (2017).
15. J.J. Chen, Y. Guo, B. Liang, et al., A radiation hardened bandgap reference voltage source. Chinese Patent CN202310904971 (2023).
16. Y.F. Hu, Z.Y. Wang, Y.Y. Yang, et al., A total-dose radiation-resistant bandgap reference voltage source. Microelectron. **52**(4), 562-565 (2022).
17. H. Zheng and A. Liang, A high-precision bandgap reference circuit for FPGA. Electron. Manuf. **31**(4), 16-19+120 (2023).
18. Y. Shi, et al., Frequent Power-Up-and-Down-Induced Degradation of Device and Bandgap Voltage Reference in 14-nm FinFET Technology. Electronics **13**(17), 3506 (2024).